Otoconin-22, the Major Protein of Aragonitic Frog Otoconia, Is a Homolog of Phospholipase A_2[†]

Kenneth G. Pote,[*,‡,§] Charles R. Hauer III,[‖] Hanspeter Michel,[‖] Jeffrey Shabanowitz,[‖] Donald F. Hunt,[‖] and Robert H. Kretsinger[‡]

Department of Biology and Department of Chemistry, University of Virginia, Charlottesville, Virginia 22901

Received May 8, 1992; Revised Manuscript Received January 4, 1993

ABSTRACT: Otoconia are composites of proteins and inorganic crystals formed in the peripheral portion of the vestibular system of vertebrates. They add mass to the extracellular otoconial membrane, thereby increasing its deflection during linear acceleration. This added mass increases the sensitivity of the underlying sensory maculae. Otoconia provide a promising system to decipher the interaction of protein and mineral during the growth and maintenance of biominerals. We have purified the major protein of the aragonitic otoconia of *Xenopus laevis*, which we call otoconin-22, and determined its amino acid sequence and carbohydrate composition. The 127 residues are 37% identical to the phospholipase A_2 from *Crotalus atrox*. We propose that otoconin-22 from *X. laevis* is homologous to phospholipase A_2 and has a similar tertiary structure.

The sensory detectors within the inner ears of vertebrates have a variety of morphologies built on a common theme: a sensory hair cell with an accessory, extracellular structure to increase the sensitivity to the end-organ's specific modality. These accessory structures are the tectorial membrane in the cochlea, the cristae in the apullae, and the otoconial membrane in the maculae. They enhance, respectively, the detection of sound, of angular acceleration, and of linear acceleration by the underlying, hair cell-containing sensory epithelium. Above the maculae of the saccule and utricle, the otoconial membranes contain small crystals of calcium carbonate known as otoliths (ear stones) if there is a single deposit or as otoconia (ear dust) if there are many. Three crystal polymorphs of $CaCO_3$ are found in otoconia and otoliths in a phylogenetically distinct pattern. Vaterite is present in otoconia of chondrostean fishes, aragonite in otoliths of holostein fishes, calcite in otoconia of mammals and birds, and both aragonite and calcite in those of reptiles and amphibians (Carlström, 1963; Marmo et al., 1983; Pote & Ross, 1991). For all three, the morphology observed in the inner ear differs somewhat from that of the $CaCO_3$ crystals grown in vitro. Figure 1 shows a micrograph of otoconia found over the saccular macula of the African clawed frog *Xenopus laevis*.

Many biominerals contain protein inferred to regulate the initiation of crystal growth and/or the subsequent rates of growth of various crystal faces. This determines the morphology and size of the final crystal (Lowenstam & Weiner, 1989). Each mineral polymorph of otoconia has a protein unique to that polymorph. Pote and Ross (1986, 1991) showed that the major protein of calcitic otoconia in mammals and amphibians has a molecular weight of 90 000 while that of the vateritic otoconia from the gar pike has a molecular weight of 54 000. The aragonitic polymorph from several species of amphibian was shown to have a major protein of 22 000 molecular weight according to mobilities on acrylamide gels. We propose the name otoconin for this class of proteins. We have characterized the protein of the aragonitic otoconia of *X. laevis* to study its developmental expression and the interactions between protein and mineral in these unique biominerals. We describe here the homology of otoconin-22 with the phospholipase A_2 family.

MATERIALS AND METHODS

The saccule of *X. laevis* contains aragonitic otoconia; it is easily dissected free of the utricle, which contains calcitic otoconia (Pote & Ross, 1986, 1991). Figure 1 shows a scanning electron micrograph of saccular otoconia. Saccular otoconia were dissected from 100 recently postmetamorphic *X. laevis* as described by Pote and Ross (1991) and washed 3 times in 0.1% sodium dodecyl sulfate (SDS) in 100 mM sodium acetate, pH 7.4. To free the protein contained within the mineral, the otoconia were demineralized in 100 mM ethylenediaminetetraacetic acid (EDTA) at 4 °C. This solution was dialyzed overnight against several changes of 10 mM $MgCl_2$ followed by eight changes of deionized H_2O. The dialysate was lyophilized and dissolved in a minimal amount of double-distilled, deionized water, and the protein concentration was measured by Bradford microassay using the protocol supplied with the reagent purchased from Bio-Rad. The lyophilized proteins were dissolved in 0.1% trifluoroacetic acid (TFA) in water and purified by high-pressure liquid chromatography (HPLC) on a C-8 reverse-phase column using the gradient described in Figure 2B. The major protein of the aragonitic otoconia, otoconin-22, was purified and its amino acid sequence determined as illustrated in Figures 2–5. The protein was reduced and S-ethylpyridinylated in 2-nmol portions dissolved in 100 μL of a thoroughly degassed solution of 8 M urea, 10 mM ethylene glycol bis(β-aminoethyl ether)-*N*,*N*,*N*′,*N*′-tetraacetic acid (EGTA), and 50 mM ammonium bicarbonate buffer, pH 8.2. Disulfide bonds were reduced by addition of 4 μL of a degassed solution of dithiothreitol (100 nmol/μL). The sample was flushed with N_2 and heated in a 50 °C sand bath for 2 h. The reduced protein was then

[†] This work is supported by National Institutes of Health Grants R29DC00929-01 (to K.G.P.) and GM37537 (to D.F.H.), by National Science Foundation Grant DMB-8917285 (to R.H.K.), and by instrument development funds from the Monsanto Co. and the National Science Foundation (to D.F.H.). K.G.P. was a NASA research associate supported by Grant NAGW-70.

[*] To whom correspondence should be addressed.

[‡] Department of Biology.

[§] Present address: Department of Otolaryngology and Communication Disorders, Harvard Medical School, Children's Hospital, 1173 Enders Building, 300 Longwood Ave., Boston, MA 02115.

[‖] Department of Chemistry.

0006-2960/93/0432-5017$04.00/0

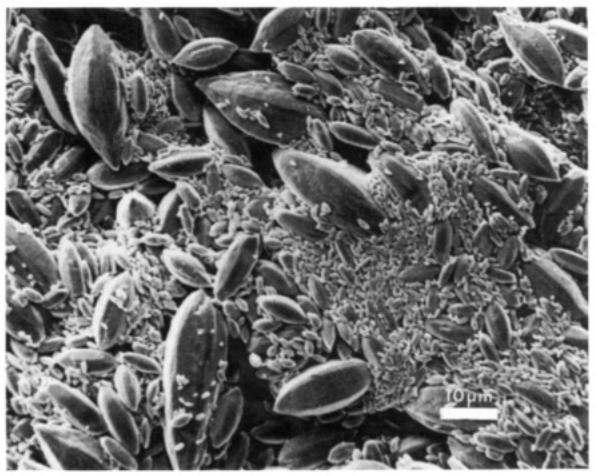

FIGURE 1: Scanning electron micrograph of saccular otoconia dissected from 100 recently postmetamorphic *Xenopus laevis* saccular otoconia.

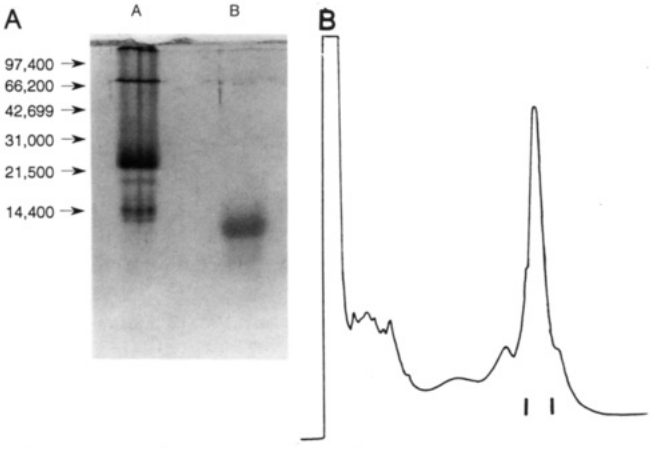

FIGURE 2: (A) Sodium dodecyl sulfate–15% polyacrylamide gel of a crude otoconial protein preparation (lane A) and a tryptic peptide collected from the preparation shown in Figure 3A. (B) Elution profile of a 22–42% gradient of buffer A (0.1% TFA in water) to buffer B (0.085% TFA in acetonitrile) over 40 min at a flow rate of 200 μL/min on an Applied Biosystems Model 130A HPLC instrument and a narrow-bore RP-300 (C-8) reverse-phase column. Over 90% of the otoconial proteins elute in one peak at 33% buffer B. The center fraction of the otoconin-22 peak indicated by the tic marks under the chromatograph was collected and lyophilized. The otoconia from 100 animals yield approximately 250 μg of otoconin-22 purified by reverse-phase HPLC.

S-ethylpyridinylated with 5 mmol of 4-vinylpyridine added in 1 μL of degassed water, for 30 min at 37 °C. Other samples of the protein were reduced and carboxymethylated in 500-pmol portions in 50 μL of degassed 0.3 M sodium sulfite, 8 M urea, 10 mM EGTA, and 100 mM Tris, pH 8.5, at 37 °C for 15 min. This yields S–SO_3^- and S^- which were carboxymethylated in the dark for 30 min at 37 °C after the addition of 5 μL of 0.298 mg of iodoacetate/100 μL of degassed water containing enough Tris-HCl to give a pH >7. The solution was then lyophilized and dissolved in 5 μL of 100 mM Tris, and unreacted disulfide bonds were reduced with 5 μL of 0.493 mg of dithiothreitol/100 μL of degassed water. This reaction was carried out under N_2 at 37 °C for 30 min. The modified protein was purified on a C-8 reverse-phase column as described in Figure 2B. Four such protein preparations were required to determine the entire sequence of otoconin-22. Two peptides that gave single blank cycles on the Edman sequenator were purified by reverse-phase HPLC for carbohydrate analysis. Approximately 500 pmol was hydrolyzed in 200 μL of 4 M trifluoroacetic acid (TFA) at 100 °C for 4 h. Approximately 75 pmol of each sample was injected into a Dionex BioLC with electrochemical detection. In addition, these glycopeptides were analyzed for molecular mass by electrospray ionization mass spectrometry (Hunt et al., 1991).

The amino acid sequence, shown in Figure 5, was used to search the National Biomedical Research Foundation (NBRF) protein data bank using FASTA (Pearson & Lipman, 1988). The otoconial protein has 37% identity with several phospholipases A_2. For this discussion, we will used the numbering system described in Figure 6. The first number will be the absolute sequence number of otoconin-22 and the second parenthetical number that of the aligned sequences in Figure 6. When the discussion concerns the phospholipase A_2 homolog family, the numbering of Figure 6 will be used. The crystal structures of both *Bos taurus* pancreatic and *Crotalus atrox* venom phospholipases A_2 have been determined and refined with high-resolution X-ray diffraction data (*B. taurus*, Dijkstra et al., 1981; *C. atrox*, Brunie et al., 1985). A model of the tertiary structure of *X. laevis* otoconin-22 was built on the coordinates for the α-carbon backbone of the Western diamond back rattlesnake (*C. atrox*) venom phospholipase A_2 (Renetseder, 1985). The amino acid side chains were altered to that of otoconin-22, and insertion of residues Ala54-(55), Glu(55(55), Phe68(70), Met79(81), and Leu117(120) was made using Sybyl software from Tripos Associates, Inc. (St. Louis, MO). The coordinates of the resulting structure were refined with 160 cycles of the Amber energy minimization program from the School of Pharmacy, University of California, San Francisco (Weiner & Kollman, 1981).

RESULTS AND DISCUSSION

N-Terminal Edman degradation was initially performed on intact, unreduced otoconin-22. Blanks were obtained at positions 20(21), 26(27), and 28(29). Position 20(21) was shown to be an asparagine with N-glycosylation while 26(27) and 28(29) were shown to be cysteine residues by mass spectrometric sequencing of the reduced and pyridylethylated protein. This may indicate cysteines in disulfide linkage, inferred to be the equivalent of Cys26–Cys122 and Cys28–Cys44 in the phospholipases A_2 (Figure 6B). This observation is consistent with extensive CNBr digestion of the unreduced protein producing low yields of peptides. Phospholipases A_2 are stable because of the multiple disulfide cross-links; our preliminary observations of otoconin-22 also indicate great stability. The similarity of the N-terminal portion of otoconin-22 with phospholipase A_2 led us to increase the amount of dithiothreitol used for reduction, thereby allowing increased internal hydrolytic cleavage by proteases.

The extracellular phospholipases examined from mammalian pancreas and snake venom form one large homolog family. A standardized numbering system for the phospholipases has been adopted to accommodate insertions (Renetseder et al., 1985) and recently expanded to include new sequences (Davidson & Dennis, 1990). There are two groups of phospholipases A_2; both have seven disulfide bonds, six of which are common as shown in Figure 6B. The amino acid sequence of otoconin-22 (Figures 1 and 2) is 127 residues long and is assigned to class II because it lacks Cys at position 11. It has all the other cysteines in the same relative positions as the class II phospholipases A_2. The alignment of otoconin-22 with several phospholipases A_2 is shown in Figure 6A. Forty-seven of the 127 (37%) residues of *X. laevis* otoconin-22 are identical to that of phospholipase A_2 from *C. atrox*. Further, of the 18 residues conserved across all sequenced phospho-

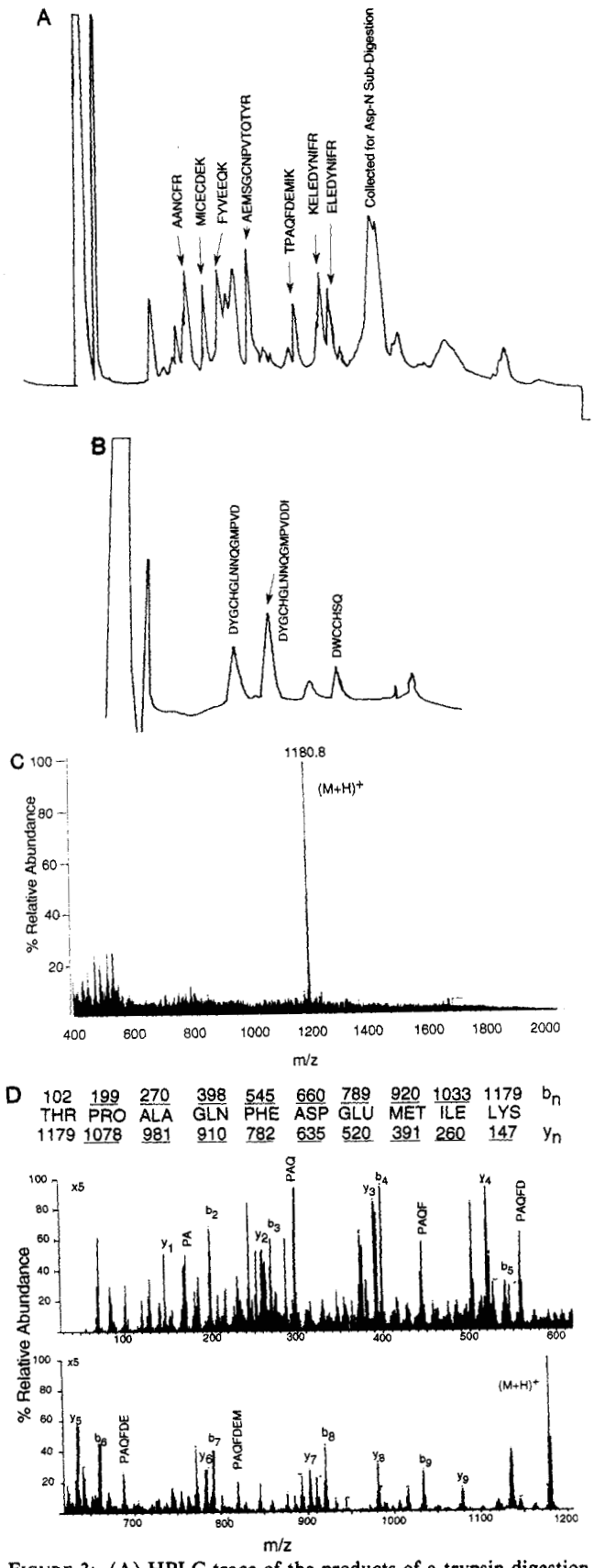

FIGURE 3: (A) HPLC trace of the products of a trypsin digestion of HPLC-purified otoconin-22. The sequences were assigned to the peaks by mass spectrometric sequence determination as illustrated by the following example. (B) HPLC trace of an endoprotease subdigestion of the peak labeled in (A). (C) Mass spectrogram of the peak labeled TPAQFDEMIK in panel A. (D) Products and amino acid sequence from a collision-activated dissociation experiment of the peptide. Underlined residues indicate observed ions.

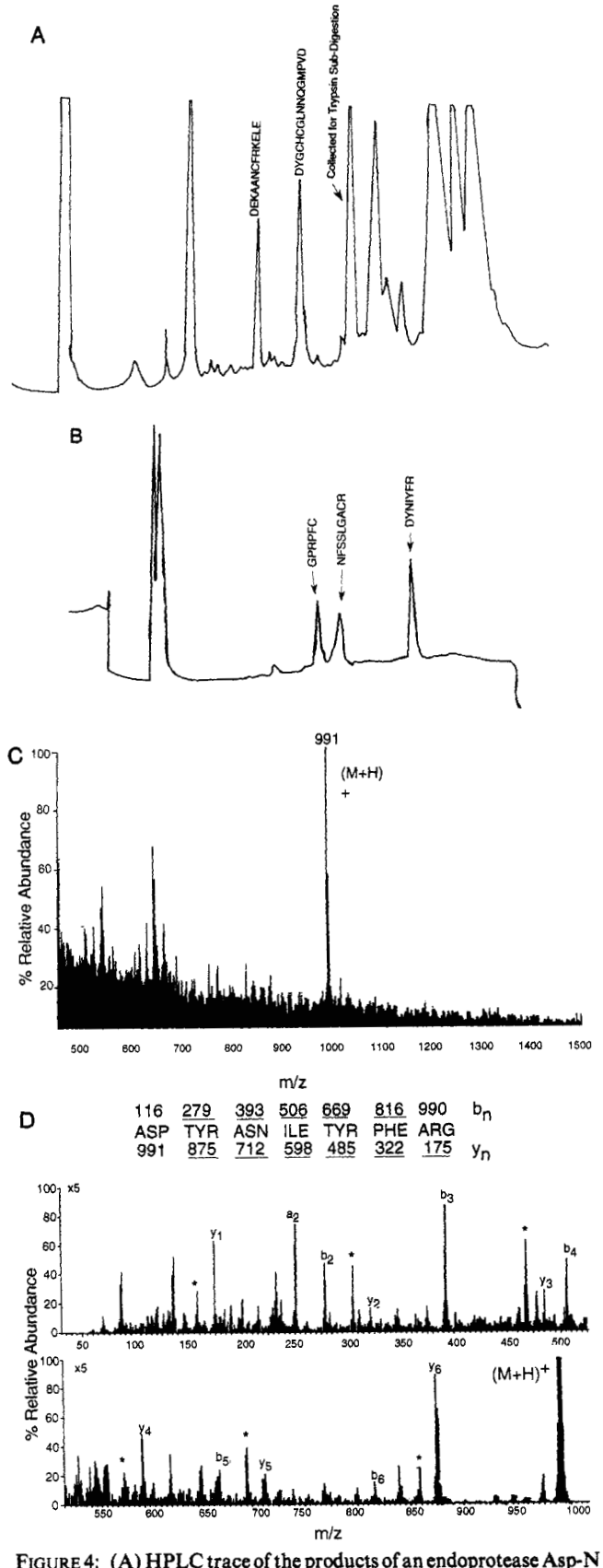

FIGURE 4: (A) HPLC trace of the products of an endoprotease Asp-N digestion of HPLC-purified otoconin-22. (B) HPLC trace of the products of trypsin subdigestion of the peak labeled in panel A. (C) Mass measurement of the peptide labeled DYNIYFR in panel B. This peptide was subjected to collision-activated dissociation. The products are illustrated in panel D along with the amino acid sequence with the masses of the peptide fragments. Isoleucines were identified by subsequent Edman degradation of the peptide. Underlined residues indicate observed ions. Asterisks indicate NH_3 loss.

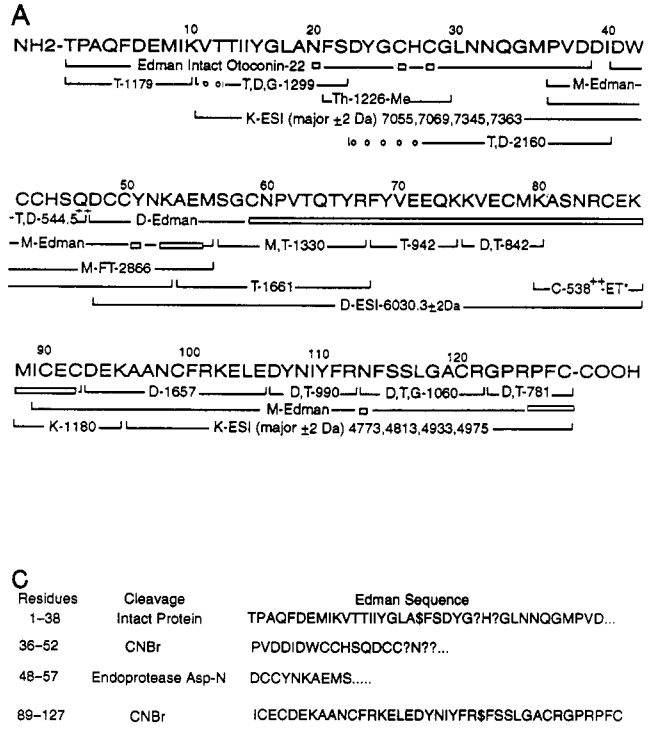

B

Cleavage	Subdigest Method	$(M+H)^+$	Residues	Sequence
Trypsin	None	1179	1–10	TPAQFDEMIK
		7062*	11–53	{VTTIIYGLA$FSDYGCHCGLNNQ GMPVDDIDWCCHSQDCCYNK}
	Endoprotease Asp-N	1932	23–38	DYGCHCGLNNQGMPVD
		2160	23–40	DYGCHCGLNNQGMPVDID
		1088*	41–47	DWCCHSQ
	None	1661	54–67	AEMSGCNPVTQTYR
		942	68–74	FYVEEQK
		842	75–80	KVECMK
		1180	88–95	MICECDEK
		786	96–101	AANCFR
		1489	102–112	KELEDYNIYFR
		1361	103–112	ELEDYNIYFR
		2824, 2868**	113–121	{$FSSLGACR}
		781	122–127	GPRPFC
Endoprotease Lys-C	None	1179	1–10	TPAQFDEMIK
		7062*	11–53	{VTTIIYGLA$FSDYGCHCGLNNQGM PVDDIDWCCHSQDCCYNK}
		2584	55–74	AEMSGCNPVTQTYRFYVEEQK
		842	75–80	KVECMK
		1180	88–95	MICECDEK
		914	96–102	AANCFRK
		4928, 4976*	103–127	{ELEDYNIYFR$FSSLGACRGPRPFC}
	Trypsin	1361	103–112	ELEDYNIYFR
		2824,2868	113–127	$FSSLGACRGPRPFC
		781	122–127	GPRPFC
CNBr	None	890	1–8	TPAQFDEM
		2866	36–56	{PVDDIDWCCHSQDCCYNKAEM}
		2905	57–79	{SGCNPVTQTYRFYVEEQKKVECM}
	Trypsin	1331	57–67	SGCNPVTQTYR
		942	68–74	FYVEEQK
Alpha-Chymotrypsin	None	536	81–87	ASNRCEK

C

Residues	Cleavage	Edman Sequence
1–38	Intact Protein	TPAQFDEMIKVTTIIYGLA$FSDYG?H?GLNNQGMPVD...
36–52	CNBr	PVDDIDWCCHSQDCC?N??...
48–57	Endoprotease Asp-N	DCCYNKAEMS.....
89–127	CNBr	ICECDEKAANCFRKELEDYNIYFR$FSSLGACRGPRPFC

FIGURE 5: Amino acid sequence data for otoconin-22 obtained by a combination of tandem mass spectrometry and Edman degradation. Peptides are labeled according to the method used to generate them and the technique used to sequence them. An asterisk indicates that cysteine has been carboxymethylated. In all other cases, cysteines have been converted to ethylpyridine derivatives. Proteolytic cleavage methods are designated as follows: K = endoprotease Lys-C; T = trypsin; C = α-chymotrypsin; D = endoprotease Asp-N; G = *N*-glycanase; Th = thermolysin; M = cyanogen bromide. The source of all enzymes was Boehringer Mannheim, Indianapolis, IN, and they were used as delivered. CNBr was purchased from Aldrich Chemical, Milwaukee, WI. These cleavage methods preceded purification by reverse-phase HPLC with a 1–100% gradient of the above described buffers. Either peptides sequenced by the technique of collision-activated dissociation (CAD) on the Finnigan-MAT, TSQ-70, triple stage quadrupole mass spectrometer (San Jose, CA) (Hunt et al., 1986, 1991) are labeled by the nominal monoisotopic mass of the corresponding $(M+H)^+$ ion if particle bombardment with cesium ions was used to ionize the sample (Hunt et al., 1986) or the mass and charge of the ion subjected to CAD is used as a label if the sample was ionized by electrospray ionization (ESI) (Hunt et al., 1991). Unidentified residues are designated by open circles. The abbreviations Et and Me indicate that the sequences were determined from CAD spectra recorded on ions from the ethyl and methyl esters of the peptide samples, respectively. Sequences confirmed by enzyme specificity and molecular mass measurements are indicated by dashed lines and one of the following labels: FT or ESI followed by the average mass of the corresponding peptide $(M+H)^+$ ion. The FT label indicates that the mass measurement was recorded under particle bombardment conditions on a Fourier transform instrument. ESI indicates that the mass was measured under electrospray ionization conditions on the triple quadrupole instrument (Hunt et al., 1987). (B) Mass assignments of peptides generated by various cleavage methods and sequences determined by collision-activated dissociation experiments. An asterisk indicates the mass was measured by ESI, and a double asterisk indicates measurement by a Fourier transform instrument. (C) Peptides sequenced by Edman degradation using an Applied Biosystems Model 473 sequenator are labeled with question marks representing unidentified residues. Amino acid assignments were determined by manual interpretation of HPLC traces of the phenylthiohydantoin (PTH) derivatives obtained from a strip chart recorder or an Apple II SE-30 computer with a software package supplied by ABI.

lipases A_2, 16 are found in the same position in otoconin-22. An interesting feature of this alignment is the presence of Ala54(55) and Glu55(56) in otoconin-22 as in many type I phospholipases A_2. We have generated phylogenetic dendrograms from the phospholipases A_2 aligned with Feng and Doolittle's (1987) progressive sequence alignment program using the methods from the recent study by Davidson and Dennis (1990) with the inclusion of the sequence for otoconin-22. Such an analysis places otoconin-22 at the root of the dendrogram prior to divergence of type I and type II phospholipases A_2. Although the alignments of the cysteines more closely resemble the type II, the presence of Ala54(55) and Glu55(56) in otoconin-22 could explain the placement of otoconin-22 as ancestral to PLA_2 types I and II by this analysis. If the sequence of a phospholipase A_2 is used to search the NBRF protein data bank, the sequence identity to other known phospholipases can be as low 45%. Given the precedents of many other homolog families, 37% identity strongly implies homology. It is frequently observed that the tertiary structures of homologous proteins can be superimposed over the region(s) of sequence similarity. Hence, it should be rewarding to examine the structures and functional characteristics of the phospholipases A_2 to focus our future investigations of otoconin-22.

Periodic acid Schiff staining of otoconial membranes shows that the otoconial proteins of *Rattus norvegicus* might be glycosylated (Belanger, 1960). In contrast, no vertebrate phospholipase A_2 is known to be glycosylated. Phospholipase A_2 from honeybee venom is glycosylated, however (Weber et al., 1986, 1987; Marz et al., 1983). The *X. laevis* otoconin-22 protein is glycosylated at Asn20(21) and Asn113(116) which consistently give blank cycles in the Edman sequenator. This is true following extensive reduction with dithiothreitol, indicating the missed residues are not cross-linked cysteines. The residues have been identified as asparagines using mass spectrometry. We have analyzed the intact protein, as well as the peptides containing Asn29(21) and Asn113(116), for carbohydrate content. The intact protein contains galactose, mannose, fucose, *N*-acetylgalactosamine, *N*-acetylglucosamine, and sialic acid (see Figure 7). Electrospray ionization mass spectra of the charged ions of the tryptic peptide containing Asn20 (residues 11–53) and the endoprotease Lys-C-generated peptide containing Asn113 (residues 103–127) consisted of multiple lines indicating various incremental masses. Many

A

```
                                     1         2         3         4         5         6    6
                            1        0         0         0         0         0         0    5
Naja naja atra              NLYQFKNMIQCTVPSR-SWWDFADYGCYCGRGGSGTPVDDLDRCCQVHDNCYNEAEKISGCWPYF
Hemachatus haemachatus      NLYQFKNMIKCTVPSR-SWWHFANYGCYCGRGGSGTPVDDLDRCCQTHDNCYSDAEKISGCRPYF
Aspidelaps scutatus         NLYQFKNMIQCTVPNR-SWWHFADYGCFCGYGGSGTPVDELDRCCQTHDNCYSEAEKLSGCKPYI
Bos taurus                  ALWQFKGMIKCKIPSSEPLLDFNNYGCYCGLGGSGTPVDDLDRCCQTHDNCYSEAEKLSGCKPYT
Crotalus adamanteus         SLVQFETLIMKVAKRS-GLLWYSAYGCYCGWGGHGRPQDATDRCCFVHDCCYGK---ATNCNPKT
Agkistrodon halys pallas    SLIQFETLIMKVAKKS-GMFWYSNYGCYCGWGGQGRPQDATDRCCFVHDCCYGK---VTGCDPKM
Trimeresurus flavoviridis   GLWQFENMIIKVVKKS-GILSYSAYGCYCGWGGRGKPKDATDRCCFVHDCCYGK---VTGCNPKL
Crotalus atrox              SLVQFETLIMKIAGRS-GLLWYSAYGCYCGWGGHGLPQDATDRCCFVHDCCYGK---ATDCNPKT
Otoconin-22                 TPAQFDEMIKVTTIIY-GLANFSDYGCHCGLNNQGMPVDDIDWCCHSQDCCYNKAE-MSGCNPVT
                                    *               **  ** •         • **  ** **  1

                                                              1         1         1          1
                            6   7         8         9         0         1         2          3
                            6   0         0         0         0         0         0          1
Naja naja atra              KTYS-YECSQGTLTCKGGNNCAAAAVCDCDRLAAICF--AGAPYN-DNDYNINLKARC-QE-----
Hemachatus haemachatus      KTYS-YDCTKGKLTCKEGNNECAAFVCKCDRLAAICF--AGAHYN-DNNNYIDLARHC-Q------
Aspidelaps scutatus         KTYS-YDCSQGKLTCSGNDDKCAAFVCNCDRVAAICF--AGAPYI-DDNYNVDLNERC-Q------
Bos taurus                  NNYS-YSCSNNEITCSSENNACEAFICNCDRNAAICF--SKVPYN-KEHKNLD-KKKC-------
Crotalus adamanteus         VSYT-YSEENGEIVC-GGDDPCGTQICECDKAAAICFRDNIPSYD-NKYWLFP-PKDC-RQEPEPC
Agkistrodon halys pallas    DVYSF-SEENGDIVC-GGDDPCKKEICECDRAAAICFRDNLTLYNDKKYWAFG-AKNCPQEESEPC
Trimeresurus flavoviridis   GKYT-YS-WQGNIVC-GGDDPCDKEVCECDRAAAICFRDNLDTYDRNKYWRYP-ASNC-QEDSEPC
Crotalus atrox              VSYT-YSEENGEIIC-GGDDPCGTQICECDKAAAICFRDNIPSYD-NKYWLFPP-KDC-REEPEPC
Otoconin-22                 QTYRFYVEEQKKVECMKASNRCEKMICECDEKAANCFRKELEDYN-IYFRNFSSLGAC-RGPRPFC
                              * 2         *3          •        •       *          4
```

B. Disulfide cross links in Phospholipase A2 and proposed in otoconin-22

Numbering in panel A	11-73	27-123	29-45	44-101	50-131	51-94	61-87	80-92
Class I	+	+	+	+		+	+	+
Class II		+	+	+	+	+	+	+
Otoconin-22 sequence number		26-120	28-44	43-99	49-127	50-92	59-85	78-90

FIGURE 6: (A) Alignments of otoconin-22 from *Xenopus laevis* with representative phospholipases A_2 of classes I and II. These sequences were extracted from the NBRF protein data bank using FASTA (Pearson & Lipman, 1988) and aligned by a progressive multisequence alignment program (Feng & Doolittle, 1987). The first four phospholipase A_2 sequences are of type I; the next five are of type II. Noteworthy is the agreement of alignment of the cysteines (C) of otoconin-22 and the type II phospholipases. Shaded boxes show identical residues for this alignment. Asterisks are placed under residues present in all sequenced phospholipases A_2 (Davidson & Dennis, 1990). Otoconin-22 contains 16 of these 18 residues. The single numbers under the sequences show the four sites into which residues were inserted into the α-carbon backbone of *Crotalus atrox* phospholipase A_2 to model the structure of otoconin-22 shown in Figure 8. (B) Cysteine disulfide cross-links are shown using the numbering of Figure 2A. This family is characterized by seven cross-links, six of which are common to class I and class II. From the alignments in panel A, the otoconial protein is most similar to the phospholipases A_2 of class II. This is most easily assessed by the absence of Cys11. The absolute sequence numbers for the proposed disulfide cross-links are shown for otoconin-22.

of these increments are equivalent to the addition of either a hexose or an *N*-acetyl group. Carbohydrate structures consistent with these data are shown in Figure 7F. These results are consistent with chemical analyses of the carbohydrate composition. From this, we assume the protein is heterogeneously glycosylated. This assumption is consistent with this protein's migration as a wide band on a polyacrylamide gel indicative of multiple size and/or charge variants. This is true whether the protein is electrophoresed in the presence or absence of SDS and reducing agents (Pote, 1987). The molecular weight of 22 000 was inferred from SDS–PAGE mobility. The amino acid sequence accounts for the 14 614 molecular weight, while the carbohydrate adds a minimum of 3800 molecular weight.

The demonstration that otoconin-22 is a glycoprotein is important because many authors have shown that otoconia formation requires proteoglycan synthesis in the otoconial membrane. This stems from Belanger's (1960) demonstration of ^{35}S incorporation into otoconial membranes indicating the presence of sulfated proteoglycan. In addition, there are many coat color mutations in mammals that also have malformed or no otoconia. Several authors (Erway et al., 1970; Shrader et al., 1973; Erway, 1986) discovered that maternal manganese supplementation can restore fetal otoconia production. The assumption was made that since manganese is a cofactor for many of the enzymes required for proteoglycan synthesis, the inability to form otoconia is a consequence of proteoglycan not being synthesized. The coat color mutant mammals have an otoconin of 90 kDa (Pote & Ross, 1986, 1991). This protein has not been sequenced nor has its carbohydrate composition been determined. If extrapolation from the aragonitic otoconial glycoprotein is valid, the other otoconins may well be expected to be glycoproteins and not proteoglycans. The mineralization mechanism may require proteoglycan synthesis for proper otoconial morphogenesis, but the otoconial protein matrix is probably made up of glycoprotein. In *X. laevis*, the glycoprotein otoconin-22 accounts for approximately 90% of the protein within the aragonitic otoconia.

The proposed backbone α-carbon trace of otoconin-22 is compared to that of *C. atrox* phospholipase A_2 in Figure 8. The alignment used for replacement of the side chains and insertions and deletions is shown Figure 6A. The insertion of Ala54(55), Glu55(56), Phe68(70), Met79(81), and Leu117-(120) occurs at the ends of loops and causes little alteration in the course of the remainder of the main chain. Unacceptable van der Waals contacts could be relieved with small movements of the side chains and almost no movement of the main chain. The sites of carbohydrate attachment are also shown in Figure 8. Both carbohydrate chains are on one side of the molecule near the ends of two adjacent loops.

A. Whole Protein Carbohydrate Analysis

Sugar	Raw Data	#	Incremental Mass	Weight in Protein
Fucose	1.9	2	147	294
Gal-NAc	2.6	3	204	612
Glc-NAc	13.1	13	204	2652
Galactose	8.7	9	163	1467
Mannose	6.8	7	163	1141
NANA	2.8	3	291	873
			Total	7039

B. Glycopeptide Carbohydrate Analysis

Sugar	Asn 113 (1)	Asn 113 (2)	Asn 20	Total	Weight in Protein
Fucose	1.0/1.0/1.0	1.0/1.0/1.0	1.0/1.0/1.0	2	294
Gal-NAc	1.0/1.0/1.0	1.0/1.0/1.0	1.0/1.0/1.0	2	408
Glc-NAc	3.1/4.6/4.0	3.8/5.6/4.0	4.0/8.0/6.0	10	2040
Galactose	2.4/2.6/3.0	2.6/2.9/3.0	3.1/5.2/4.0	7	1141
Mannose	2.2/3.0/3.0	2.7/3.0/3.0/	4.5/7.9/6.0	9	1467
NANA	N.D.	N.D.	N.D.	N.D.	N.D.
				Total	5350

F. Proposed carbohydrate side chains on otoconin-22

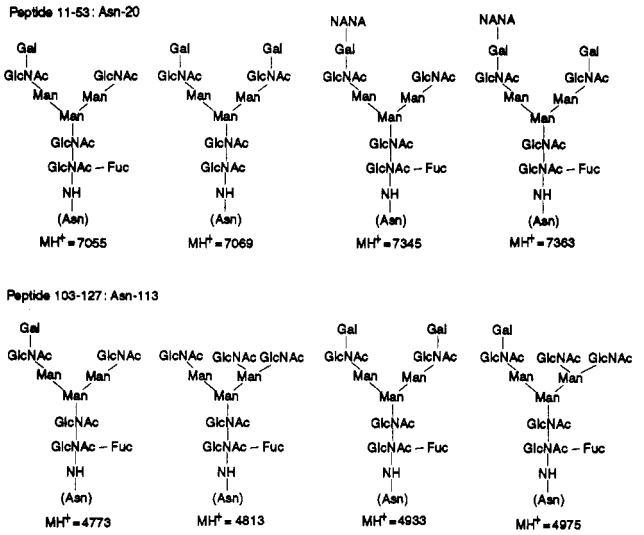

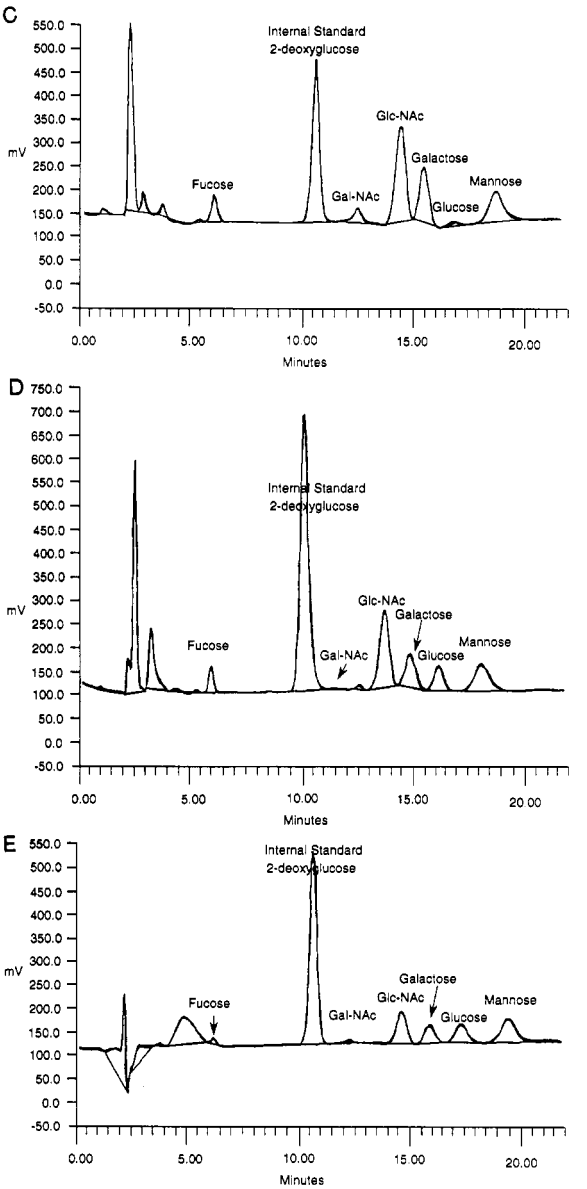

FIGURE 7: (A) Summary of results of carbohydrate analyses of HPLC-purified, intact *Xenopus laevis* otoconin-22. The purified protein was analyzed for carbohydrate using a Dionex BioLC and quantified using internal standards. Abbreviations: GalNAc, *N*-acetylgalactosamine; NANA, *N*-acetylneuraminic acid (sialic acid); Man, mannose; Fuc, fucose; Gal, galactose; GlcNAc, *N*-acetylglucosamine. There is general agreement in the total sugar present and that present in each glycopeptide. Sugar represents approximately 34% of the mass of the glycoprotein from these measurements. (B) Carbohydrate analysis of HPLC-purified glycopeptides. The glycopeptide containing Asn113(116) was purified twice for carbohydrate analysis. The glycopeptide containing Asn20(21) was purified only once. All samples were run in duplicate. The three numbers for the glycopeptide analyses are the first run, the second run, and their whole number average, respectively. Abbreviations are as in Figure 3A. (C) Chromatogram of carbohydrate analysis of intact otoconin-22 after hydrolysis in 4 M trifluoroacetic acetic acid for 4 h. Abbreviations are as in Figure 3A. (D) Chromatogram of carbohydrate analysis of N-terminal glycopeptide following hydrolysis. Abbreviations are as in Figure 3A. (E) Chromatogram of carbohydrate analysis of C-terminal glycopeptide following hydrolysis. Abbreviations are as in Figure 3A. (F) Proposed structures of the carbohydrate side chains on otoconin-22. These structures were derived from the incremental masses of the glycopeptide analyzed by electrospray ionization mass spectrometry of the HPLC-purified glycopeptides. Abbreviations are as in Figure 3A.

Some members of class II phospholipase A_2 function as dimers and some as monomers. The dimer interface as seen in the crystal structure of *C. atrox* phospholipase A_2 has contacts involving hydrophobic side chains of residues. In *C. atrox*, Trp30 extends into a hydrophobic pocket in the other monomer to hold the monomers together. From the alignment illustrated in Figure 6, this position is a leucine in the *X. laevis* otoconin-22. There is no evidence of dimer formation when otoconin-22 is separated on a native or reducing and denaturing polyacrylamide gel. This suggests, but does not prove, that otoconin-22 is monomeric.

Most phospholipases A_2 bind a Ca^{2+} ion with a low, i.e., millimolar, affinity; it is essential for enzymatic activity. In the crystal structure from *B. taurus* (Dijkstra, 1981), calcium is coordinated by two water molecules, the carbonyl oxygen atoms of Tyr28, Gly30, and Gly32, as well as by both oxygen atoms of the carboxylate group of Asp49. Except for Tyr28, these four residues are invariant in active phospholipases A_2. In otoconin-22, two of the four corresponding residues of the calcium binding loop are altered. Tyr27(28) is replaced by His27(28), and Gly31(32) is replaced by Asn. In modeling and refinement studies, this substitution of asparagine for glycine maintains the general course of the main chain; however, the carbonyl of Asn31(32) of otoconin-22 no longer points at the putative calcium binding site. Residues His48, Asp49, and Asp95 are clearly involved in catalysis (Dijkstra

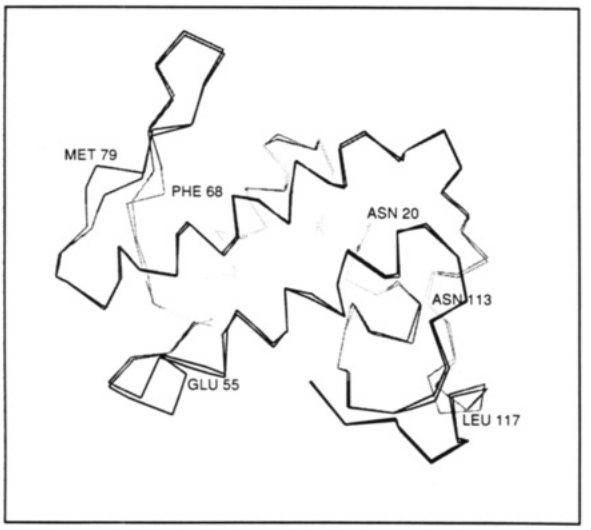

FIGURE 8: Proposed tertiary structure of otoconin-22 of *Xenopus laevis* superimposed on the backbone of phospholipase A_2 from *Crotalus atrox*. The model was built using the initial backbone coordinates of *C. atrox* phospholipase A_2 by replacing the *C. atrox* amino acids with those of otoconin-22. The insertions of residues Ala54(55), Glu55(56), Phe68(70), Met79(81), and Leu117(120) was accomplished with Sybyl software. These insertion sites are numbered at the bottom of the sequences in Figure 2A. The resulting structure was refined by energy minimization and dynamics with Sybyl. The two sites of glycosylation are shown as Asn20 and Asn113.

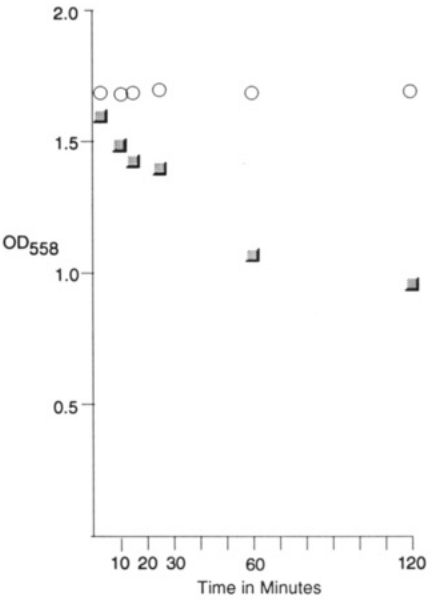

FIGURE 9: Results from a test of phospholipase A_2 activity in otoconin-22. This assay used 0.1 μg of otoconin-22 in 1 mL of 4 mM diphosphatidylcholine solubilized in 10 mM Triton X-100 micelles, 50 mM KCl, and 0.06 mM phenol red at pH 7.6, the pK of phenol red, and 1 μM Tris-HCl, pH 7.6, at room temperature. Pancreatic phospholipase purchased from Sigma (square data points) replaced otoconin-22 (open circles) in the control samples.

et al., 1981; Davidson & Dennis, 1990). Little is known about the residues involved in conformational changes that occur when the phospholipase binds to lipid bilayers. Even so, the Ca^{2+} ion is not involved in catalysis or in the binding of substrate or product. Radioactive ^{45}Ca is not bound by *X. laevis* otoconin-22 transferred to nitrocellulose (Pote & Ross, 1991).

Phospholipase A_2 is especially interesting in that its velocity of reaction is much higher when an intact lipid bilayer, rather than a single diacylglyceride, is the substrate. This implies a major change of conformation for either the enzyme or the bilayer and probably both. The inferred or determined structure of isolated otoconin-22 may be significantly different from that found in the $CaCO_3$ crystal lattice of otoconia. The catalytic activity of the phospholipases A_2 requires the presence of His56(48) which is present as Gln in otoconin-22. Given the alterations of the residues in the calcium binding loop and at the active site in otoconin-22, it is unlikely that this protein has phospholipase activity. Preliminary experiments have detected no such activity using a slightly modified spectrophotometric method of Lôbo de Araújo and Radvanyi (1987). This assay was repeated 2 times using 0.1 μg of otoconin-22 in 1 mL of 4 mM diphosphatidylcholine solubilized in 10 mM Triton X-100 micelles, 50 mM KCl, and 0.06 mM phenol red at pH 7.6, the pK of phenol red, with 1 μM Tris-HCl, pH 7.6. Control experiments were conducted using 0.1 μg of pancreatic phospholipase purchased from Sigma in place of otoconin-22, and by adding no protein. The assay was left at room temperature. The OD_{558} values of the solutions were checked several times over the course of several hours. No change in absorbance was detected in the solutions containing otoconin-22 or no protein. A decrease in absorbance could be detected within 15 min for the solutions containing the pancreatic phospholipase (see Figure 9).

The similarity of amino acid sequence between otoconin-22 from *X. laevis* and the phospholipase A_2 brings to mind the similarities of the taxon-specific lens crystallin proteins and various enzymes (Wistow & Piatigorsky, 1987; Wistow et al., 1988; Hendriks et al., 1988; Watanabe et al., 1988; Piatigorsky & Wistow, 1989). The homology of the phospholipases A_2 and otoconin-22 is another example of the eclectic nature of evolution and shows the difficulty of predicting protein function from primary structure. If one were able to replay the tape of life, as suggested by Gould (1989), one might expect different protein structure–function relationships. In other words, the selection of the structural otoconin-22 might in the replay be derived from another protein precursor.

Our studies of otoconia have two goals: determining the developmental expression of the proteins in the tissue(s) that produce otoconia and understanding the function of the otoconins in biomineralization. Our initial results using polycolonal antibodies raised against the otoconins and Western blots show that only the inner ear epithelial tissues produce the major otoconins in *Rattus norvegicus* and in *X. laevis*. Determination of the amino acid sequence and inference of the tertiary structure of the major otoconial protein from *X. laevis* is a major step toward understanding the molecular mechanism and control of biomineralization.

ACKNOWLEDGMENT

We thank E. Jane Self for editorial assistance.

REFERENCES

Belanger, L. F. (1960) in *Calcification in Biological Systems* (Sognnaes, R. F., Ed.) pp 151–162, American Association for the Advancement of Science, Washington, D.C.

Brunie, S., Bolin, J., Gewirth, D., & Sigler, P. B. (1985) *J. Biol. Chem. 260*, 9742–9749.

Carlström, D. (1963) *Biol. Bull. (Woods Hole, Mass.) 125*, 441–463.

Davidson, F. F., & Dennis, E. A. (1990) *J. Mol. Evol. 31*, 228–238.

Dijkstra, B. W., Kalk, K. H., Hol, W. G. J., & Drenth, J. (1981) *J. Mol. Biol. 147*, 97–123.

Erway, L. C., Hurley, L. S., & Fraser, A. S. (1970) *J. Nutr. 100*, 643–654.

Erway, L. C., Purichia, N. A., Netzler, E. R., D'Amore, M. A., Esses, D., & Levine, M. (1986) *Scanning Electron microsc. 4*, 1681–1694.

Feng, D. F., & Doolittle, R. F. (1987) *J. Mol. Evol. 25*, 351–360.

Gould, S. J. (1989) *Wonderful Life*, W. W. Norton and Co., New York.

Hendriks, W., Mulders, J. W., Bibby, M. A., Slingsby, C., Bloemendal, H., & de Jong, W. W. (1988) *Proc. Natl. Acad. Sci. U.S.A. 85*, 7114–7118.

Hunt, D. F., Yates, Y. R., Shabanowitz, J., Winston, S., & Hauer, C. R. (1986) *Proc. Natl. Acad. Sci. U.S.A. 83*, 6233–6237.

Hunt, D. F., Shabanowitz, J., Yates, J. R., Zhu, N.-Z., Russell, D. H., & Castro, M. E. (1987) *Proc. Natl. Acad. Sci. U.S.A. 84*, 620–623.

Hunt, D. F., Alexander, J. E., McCormack, A. L., Martino, P. A., Michel, H., Shabanowitz, J., & Sherman, N. (1991) *Techniques in Protein Chemistry II* (Villafranca, J. J., Ed.) pp 441–454, Academic Press, New York.

Lôbo de Araújo, A., & Radvanyi, F. (1987) *Toxicon 25*, 1181–1188.

Lowenstam, H. A., & Weiner, S. (1989) *On Biomineralization*, Oxford University Press, New York.

Marmo, F., Balsamo, G., & Franco, E. (1983) *Cell Tissue Res. 233*, 35–43.

Marz, L., Kuhne, C., & Michl, H. (1983) *Toxicon 21*, 893–896.

Pearson, W. R., & Lipman, D. J. (1988) *Proc. Natl. Acad. Sci. U.S.A. 85*, 2444–2448.

Piatigorsky, J., & Wistow, G. J. (1989) *Cell 57*, 197–199.

Pote, K. G. (1987) Thesis, The University of Michigan.

Pote, K. G., & Ross, M. D. (1986) *J. Ultrastruct. Mol. Struct. Res. 95*, 61–70.

Pote, K. G., & Ross, M. D. (1991) *J. Comp. Biochem. Physiol. 98B*, 287–295.

Renetseder, R., Brunie, S., Dijkstra, B. W., Drenth, J., & Sigler, P. B. (1985) *J. Biol. Chem. 260*, 11627–11634.

Shrader, R. C., Erway, L. C., & Hurley, L. S. (1973) *Teratology 8*, 257–266.

Simkiss, K., & Wilbur, K. M. (1989) *Biomineralization Cell Biology and Mineral Deposition*, Academic Press, New York.

Watanabe, K., Fujii, Y., Nakayama, K., Ohkubo, H., Kuramitsu, S., Kagakiyama, H., Nakanishi, S., & Hayaishi, O. (1988) *Proc. Natl. Acad. Sci. U.S.A. 85*, 11–15.

Weber, A., Marz, L., & Altmann, F. (1986) *Comp. Biochem. Physiol. B 83(2)*, 321–324.

Weber, A., Schroder, H., Thalberg, K., & Marz, L. (1987) *Allergy 42*, 464–470.

Weiner, P. K., & Kollman, P. A. (1981) *J. Comput. Chem. 2*, 287–303.

Wistow, G., & Piatigorsky, J. (1987) *Science 236*, 1554–1555.

Wistow, G. J., Leitman, T., Williams, L. A., Stapel, S. O., & de Jong, W. W. (1988) *J. Biol. Chem. 107*, 2729–2736.